Original Article

Cardiac-Specific Overexpression of Peroxisome Proliferator–Activated Receptor-α Causes Insulin Resistance in Heart and Liver

So-Young Park,[1] You-Ree Cho,[1] Brian N. Finck,[2] Hyo-Jeong Kim,[1] Takamasa Higashimori,[1] Eun-Gyoung Hong,[1] Mi-Kyung Lee,[1] Cheryl Danton,[1] Swati Deshmukh,[1] Gary W. Cline,[1] Julie J. Wu,[3] Anton M. Bennett,[3] Beverly Rothermel,[4] April Kalinowski,[5] Kerry S. Russell,[5] Young-Bum Kim,[6] Daniel P. Kelly,[2] and Jason K. Kim[1,7]

Diabetic heart failure may be causally associated with alterations in cardiac energy metabolism and insulin resistance. Mice with heart-specific overexpression of peroxisome proliferator–activated receptor (PPAR)α showed a metabolic and cardiomyopathic phenotype similar to the diabetic heart, and we determined tissue-specific glucose metabolism and insulin action in vivo during hyperinsulinemic-euglycemic clamps in awake myosin heavy chain (MHC)-PPARα mice (12–14 weeks of age). Basal and insulin-stimulated glucose uptake in heart was significantly reduced in the MHC-PPARα mice, and cardiac insulin resistance was mostly attributed to defects in insulin-stimulated activities of insulin receptor substrate (IRS)-1–associated phosphatidylinositol (PI) 3-kinase, Akt, and tyrosine phosphorylation of signal transducer and activator of transcription 3 (STAT3). Interestingly, MHC-PPARα mice developed hepatic insulin resistance associated with defects in insulin-mediated IRS-2–associated PI 3-kinase activity, increased hepatic triglyceride, and circulating interleukin-6 levels. To determine the underlying mechanism, insulin clamps were conducted in 8-week-old MHC-PPARα mice. Insulin-stimulated cardiac glucose uptake was similarly reduced in 8-week-old MHC-PPARα mice without changes in cardiac function and hepatic insulin action compared with the age-matched wild-type littermates. Overall, these findings indicate that increased activity of PPARα, as occurs in the diabetic heart, leads to cardiac insulin resistance associated with defects in insulin signaling and STAT3 activity, subsequently leading to reduced cardiac function. Additionally, age-associated hepatic insulin resistance develops in MHC-PPARα mice that may be due to altered cardiac metabolism, functions, and/or inflammatory cytokines. ***Diabetes*** **54:2514–2524, 2005**

Cardiovascular disease is the leading cause of mortality in type 2 diabetes (1,2). Although the etiology of diabetic heart failure is poorly understood, there is a growing body of evidence (3–5) indicating that alterations in cardiac energy metabolism may precede and be causally associated with the development of cardiomyopathy in the diabetic heart. The peroxisome proliferator–activated receptors (PPARs) are ligand-activated transcription factors belonging to the nuclear receptor superfamily, and of the three identified mammalian PPAR subtypes (α, γ, and δ), PPARα regulates nuclear expression of genes involved in lipid metabolism in various cell types including heart (6,7). Since normal cardiac function is dependent on a constant rate of ATP resynthesis predominantly driven by mitochondrial fatty acid oxidation, activation of PPARα by endogenous ligands, such as fatty acids, plays an important role in cardiac energy metabolism and functions (8,9). Mice with heart-specific overexpression of PPARα (myosin heavy chain [MHC]-PPARα) were recently shown to exhibit increased rates of myocardial lipid oxidation, consistent with the role of PPARα (10). Importantly, MHC-PPARα mice developed cardiomyopathy with enhanced sensitivity to myocardial ischemic insult, and these functional/structural changes were associated with reduced expression of genes involved in cardiac glucose utilization (10). In this regard, increased lipid oxidation and reduced glucose

From the [1]Department of Internal Medicine, Section of Endocrinology and Metabolism, Yale University School of Medicine, New Haven, Connecticut; the [2]Department of Medicine, Center for Cardiovascular Research, Washington University School of Medicine, St. Louis, Missouri; the [3]Department of Pharmacology, Yale University School of Medicine, New Haven, Connecticut; the [4]Department of Internal Medicine, University of Texas Southwestern Medical Center, Dallas, Texas; the [5]Section of Cardiology, Yale University School of Medicine, New Haven, Connecticut; the [6]Division of Endocrinology, Diabetes, and Metabolism, Beth Israel Deaconess Medical Center, Harvard Medical School, Boston, Massachusetts; and the [7]Yale Mouse Metabolic Phenotyping Center, Yale University School of Medicine, New Haven, Connecticut.

Address correspondence and reprint requests to Prof. Jason K. Kim, Yale University School of Medicine, Department of Internal Medicine, Section of Endocrinology and Metabolism, The Anlyan Center, S269C, P.O. Box 208020, 300 Cedar St., New Haven, CT 06520-8020. E-mail: jason.k.kim@yale.edu.

Received for publication 21 February 2005 and accepted in revised form 16 June 2005.

D.P.K. has received consulting fees from Pfizer Global Research and Development and Sankyo.

2-[^{14}C]DG, 2-deoxy-D-[1-^{14}C]glucose; 2-[^{14}C]DG-6-P, 2-[^{14}C]DG-6-phosphate; GSK, glycogen synthase kinase; HGP, hepatic glucose production; IL, interleukin; IRS, insulin receptor substrate; MAPK, mitogen-activated protein kinase; MHC, myosin heavy chain; PET, positron emission tomography; PI, phosphatidylinositol; PPAR, peroxisome proliferator–activated receptor; STAT3, signal transducer and activator of transcription 3.

metabolism, possibly due to increased activity of PPARα gene regulatory pathway, are characteristic features of diabetic heart (3–5). Furthermore, studies (11–13) using isolated perfused heart preparations, cultured cardiomyocytes, and positron emission tomography (PET) uniformly showed insulin resistance in human and animal models of diabetic heart. Cardiac insulin resistance was also associated with diabetes independent of coronary artery disease, hypertension, and changes in coronary blood flow (14,15). While these studies strongly demonstrate the important role of insulin resistance in diabetic heart, it is unclear whether altered cardiac insulin sensitivity is a result of increased myocardial lipid oxidation. To determine the mechanism of altered cardiac glucose metabolism, the present study examined the changes in cardiac energy metabolism, insulin action, and insulin signaling in vivo in the MHC-PPARα mice.

RESEARCH DESIGN AND METHODS

Surgery. Male MHC-PPARα mice and wild-type littermates (10) weighing ~27 g (12–14 weeks of age) were housed under controlled temperature (23°C) and lighting (12 h of light, 0700–1900; 12 h of dark, 1900–0700), with free access to water and standard mouse diet. At least 4 days before in vivo experiments, whole-body fat and lean mass were measured in awake mice using ^{1}H-magnetic resonance spectroscopy (Bruker Mini-spec Analyzer; Echo Medical Systems, Houston, TX). Following the body composition measurement, mice were anesthetized with an intraperitoneal injection of ketamine (100 mg/kg body wt) and xylazine (10 mg/kg body wt), and an indwelling catheter was inserted in the right internal jugular vein. On the day of experiment (4–5 days postsurgery), a 3-way connector was attached to the jugular vein catheter to intravenously deliver solutions (e.g., glucose, insulin). Also, mice were placed in a rat-size restrainer (to minimize stress during experiments in awake state) and tail restrained using a tape to obtain blood samples from the tail vessels. All procedures were approved by Yale University Animal Care and Use Committee.

Basal glucose and palmitate uptake in heart in vivo. Basal rates of glucose and palmitate uptake in heart were assessed in awake MHC-PPARα mice and wild-type littermates (n = 6 for both groups). Basal cardiac glucose uptake was assessed in overnight-fasted mice by intravenously bolus injecting 2-deoxy-D-[1-^{14}C]glucose (2-[^{14}C]DG; 10 μCi; PerkinElmer Life and Analytical Sciences, Boston, MA) and obtaining heart samples 30 min later for the measurement of 2-[^{14}C]DG-6-phosphate (2-[^{14}C]DG-6-P). Plasma samples were taken at 5- to 10-min intervals following injection to measure the concentrations of 2-[^{14}C]DG. Basal cardiac palmitate uptake was similarly assessed in mice by intravenously injecting [^{14}C]palmitate (10 μCi; PerkinElmer Life and Analytical Sciences) and obtaining heart samples 5 min later for the measurement of [^{14}C] incorporation into triglyceride. Plasma samples were taken at 30-s to 1-min intervals following injection to measure the concentrations of [^{14}C]palmitate.

Hyperinsulinemic-euglycemic clamps to assess insulin action in vivo. After overnight fast, a 2-h hyperinsulinemic-euglycemic clamp was conducted in awake MHC-PPARα mice and wild-type littermates (n = 6–13). The experiment began with a primed-continuous infusion of human regular insulin (Humulin; Eli Lilly, Indianapolis, IN) at a rate of 15 pmol · kg^{-1} · min^{-1} to raise plasma insulin within a physiological range (~200 pmol/l) (16). Blood samples (20 μl) were collected at 10- to 20-min intervals for the immediate measurement of plasma glucose concentration, and 20% glucose was infused at variable rates to maintain glucose at basal concentrations (~6 mmol/l). Basal and insulin-stimulated whole-body glucose uptake was estimated with a continuous infusion of [3-^{3}H]glucose (PerkinElmer Life and Analytical Sciences) for 2 h before the clamps (0.05 μCi/min) and throughout the clamps (0.1 μCi/min), respectively. All infusions were performed using the microdialysis pumps (CMA/Microdialysis, North Chelmsford, MA). To estimate insulin-stimulated glucose uptake in individual tissues, 2-[^{14}C]DG was administered as a bolus (10 μCi) at 75 min after the start of clamps. Blood samples were taken before, during, and at the end of clamps for measurement of plasma [^{3}H]glucose, ^3H_2O, 2-[^{14}C]DG concentrations, and/or insulin concentrations. At the end of the clamps, mice were anesthetized with sodium pentobarbital injection, and tissue samples (gastrocnemius, tibialis anterior, and quadriceps from both hindlimbs, epididymal white adipose tissue, interscapular brown adipose tissue, liver, and heart) were rapidly taken for biochemical and molecular analysis.

Biochemical assays and calculation. Glucose concentration during clamps was analyzed using 10 μl plasma by a glucose oxidase method on a Beckman Glucose Analyzer 2 (Beckman, Fullerton, CA). Plasma insulin concentration was measured by radioimmunoassay using kits from Linco Research (St. Charles, MO). Circulating levels of interleukin (IL)-6 were measured using an enzyme-linked immunosorbent assay kit from R&D Systems (Quantikine, Minneapolis, MN). Plasma concentrations of [3-^{3}H]glucose, 2-[^{14}C]DG, and ^3H_2O were determined following deproteinization of plasma samples as previously described (16). The radioactivity of ^{3}H in tissue glycogen was determined by digesting tissue samples in KOH and precipitating glycogen with ethanol. For the determination of tissue 2-[^{14}C]DG-6-P content, tissue samples were homogenized, and the supernatants were subjected to an ion-exchange column to separate 2-[^{14}C]DG-6-P from 2-[^{14}C]DG.

Rates of basal hepatic glucose production (HGP) and insulin-stimulated whole-body glucose uptake were determined as the ratio of the [^{3}H]glucose infusion rate (disintegrations per minute; dpm/min) to the specific activity of plasma glucose (dpm/μmol) at the end of basal period and during the final 30 min of clamps, respectively. Insulin-stimulated rates of HGP during clamps were determined by subtracting the glucose infusion rate from the whole-body glucose uptake. Whole-body glycolysis was calculated from the rate of increase in plasma ^3H_2O concentration, determined by linear regression of the measurements at 80, 90, 100, 110, and 120 min of clamps. Whole-body glycogen plus lipid synthesis from glucose was estimated by subtracting whole-body glycolysis from whole-body glucose uptake (16). Since 2-deoxyglucose is a glucose analog that is phosphorylated but not further metabolized, insulin-stimulated glucose uptake in individual tissues can be estimated by determining the tissue (e.g., skeletal muscle, heart) content of 2-[^{14}C]DG-6-P. Based on this, glucose uptake in individual tissues was calculated from plasma 2-[^{14}C]DG profile, which was fitted with a double exponential or linear curve using MLAB (Civilized Software, Bethesda, MD) and tissue 2-[^{14}C]DG-6-P content. Tissue glycogen synthesis was assessed as previously described (16).

Insulin signaling analysis. Heart and liver samples were obtained at the end of insulin clamps to measure in vivo activities of insulin receptor substrate (IRS)-1 and IRS-2–associated phosphatidylinositol (PI) 3-kinase, respectively. These activities were assessed by immunoprecipitating tissue lysates with polyclonal IRS-1/IRS-2 antibodies (Upstate Biotechnology, Lake Placid, NY) coupled to protein A-Sepharose beads (Sigma, St. Louis, MO) and assessing the incorporation of ^{32}P into PI to yield PI 3-monophosphate. The immune complex was washed, and the activity was determined as previously described (16). In additional groups of mice (n = 6 for MHC-PPARα mice and wild-type littermates), basal and insulin-stimulated insulin signaling were assessed following intraperitoneal injection of saline and insulin, respectively, and the heart samples were taken 15 min following the injection. Insulin-stimulated Akt activity was determined in heart samples obtained at the end of clamps as previously described (17). Basal Akt activities were measured in overnight-fasted MHC-PPARα mice and wild-type mice (n = 3 for each group).

Activity and expression of other signaling proteins. For the measurement of signal transducer and activator of transcription 3 (STAT3) protein expression and tyrosine phosphorylation of STAT3, heart and liver samples were obtained at the end of clamps. Sample lysates were resolved by SDS-PAGE (8% gel) and transferred to nitrocellulose membranes. The nitrocellulose membranes were blocked and incubated with phospho-specific STAT3 (Tyr705) polyclonal antibody (Cell Signaling, Beverly, MA). The membranes were washed and incubated with horseradish peroxidase secondary antibody (Amersham Pharmaceuticals, Arlington Heights, IL), and the bands were visualized using the enhanced chemiluminescence system (Amersham Pharmaceuticals). For the PPARα expression in individual organs, whole-cell protein extracts were prepared from heart and liver samples, and Western blotting studies were performed using rabbit-derived antibodies directed against the Flag epitope tag (Sigma) as previously described (18). For the p38 mitogen-activated protein kinase (MAPK) activity, heart samples were homogenized in 20 vol of homogenizing buffer (20 mmol/l Hepes, pH 7.4; 150 mmol/l NaCl; 2 mmol/l EDTA; 1% TritonX-100; 0.1% SDS; 10% glycerol; 1 mmol/l dithiothreitol; 0.5% deoxycholate, supplemented with 5 μg/ml leupeptin; 5 μg/ml aprotinin; 1 μg/ml pepstatin A; 1 mmol/l phenylmethylsulfonyl fluoride; 1 mmol/l benzamidine; 2 mmol/l Na_3VO_4; and 5 mmol/l NaF) and lysed for 30 min before clarification at 20,800g for 30 min. Protein concentration was determined by Coomassie protein reagent (Pierce, Rockford, IL). p38 MAPK was immunoprecipitated using anti-p38 MAPK antibody (Santa Cruz) and collected on protein-G Sepharose beads. The immune complexes were subjected to an in vitro kinase assay as previously described (19). Glycogen synthase kinase (GSK)3 phosphorylation was assessed by Western blot analysis using antibodies directed against phosphorylated GSK3-α/-β (SER21/9) (Cell Signaling Technologies) and total GSK3-β. A total of 20 μg protein were run on SDS-PAGE, transferred to nitrocellulose, and reacted with primary antibody and horseradish peroxidase–conjugated secondary

TABLE 1
Metabolic parameters of the wild-type and MHC-PPARα mice (12–14 weeks of age) at basal (overnight fasted) and during a 2-h hyperinsulinemic-euglycemic clamp experiment

		Body weight	Lean mass	Fat mass	Basal period		Clamp period	
	n	(g)	(g)	(g)	Plasma glucose (mmol/l)	Plasma insulin (pmol/l)	Plasma glucose (mmol/l)	Plasma insulin (pmol/l)
Wild type	6–13	27 ± 1	21 ± 1	5 ± 1	7.0 ± 0.4	86 ± 8	5.7 ± 0.3	198 ± 10
MHC-PPARα	7–13	27 ± 1	22 ± 1	4 ± 1	7.2 ± 0.3	82 ± 6	6.4 ± 0.3	178 ± 38

Data are means ± SE.

antibody. Signal was detected using enhanced chemiluminescence plus (Amersham Biosciences) and the ratio of phosphorylated to total GSK3 quantified on using a STORM 860 (Molecular Dynamics).

Measurements of triglyceride and fatty acid metabolites in heart and liver. For the measurement of tissue-specific triglyceride concentration, heart and liver samples were digested in chloroform-methanol (20). Lipid layer was separated using H_2SO_4, and concentrations were determined using triglyceride assay kit (Sigma Diagnostics) and spectrophotometry. To determine the intramyocardial and intrahepatic concentrations of fatty acid metabolites (long-chain acyl CoAs, diacylglycerol) using LC/MS/MS (liquid-chromatography tandem mass spectrometry), heart and liver samples were homogenized and extracted as previously described (21,22). Briefly, frozen tissue samples (~100 mg) were grounded under liquid nitrogen and homogenized in 1 ml of 100 mmol/l KH_2PO_4 (pH 4.9) and 1 ml of 2-propanol. Heptadecanoyl CoA was added as internal standard. A total of 125 μl saturated $(NH_4)_2SO_4$ and 2 ml acetonitrile were added to the suspension then vortexed for 2 min. The emulsion was centrifuged for 10 min at 4,000 rpm, and then the supernatant was diluted with 5 ml of 100 mmol/l KH_2PO_4 (pH 4.9) for the solid-phase extraction. Before the loading, oligonucleotide purification cartridge columns were conditioned with 5 ml acetonitrile and 2 ml of 25 mmol/l KH_2PO_4 (pH 4.9). After loading the samples, the cartridges were washed with at least 10 ml distilled H_2O, and then long-chain acyl CoAs were eluted slowly with 0.5 ml of 60% acetonitrile. The eluent was dried in Speedvac and finally reconstituted in 100 μl methanol/H_2O for ESI/MS/MS (electrospray ionization tandem mass spectrometry) analysis.

PerkinElmer sciex API 3000 tandem mass spectrometer interfaced with TurboIonSpray ionization source was used for the analysis. The intracellular concentrations of long-chain fatty acyl CoAs (C16:0, C16:1, C18:0, C18:1, C18:2, and C18:3) were detected in negative electrospray mode. The doubly charged ions of these compounds were transmitted, and singly charged product ions were quantified in multiple reaction mode. Long-chain acyl CoA standards were purchased from Sigma Chemical (St. Louis, MO). The calibration of long-chain acyl CoAs showed consistent linearity from 0.2 to 20 ng/μl, and coefficient of variance was 2.1–5.5% for all long-chain acyl CoA species. The intracellular concentrations of diacylglycerol were measured as previously described (20).

Echocardiography to assess cardiac function. M-mode echocardiography was performed in additional groups of age-matched MHC-PPARα mice and wild-type littermates (n = 5 for both groups) using the Phillips Sonos 5500 System with a 15-MHz probe. Mice were lightly anesthetized with inhaled isoflurane, and images were collected in the short and long axis. Data represents the averaged values of 3–5 cardiac cycles.

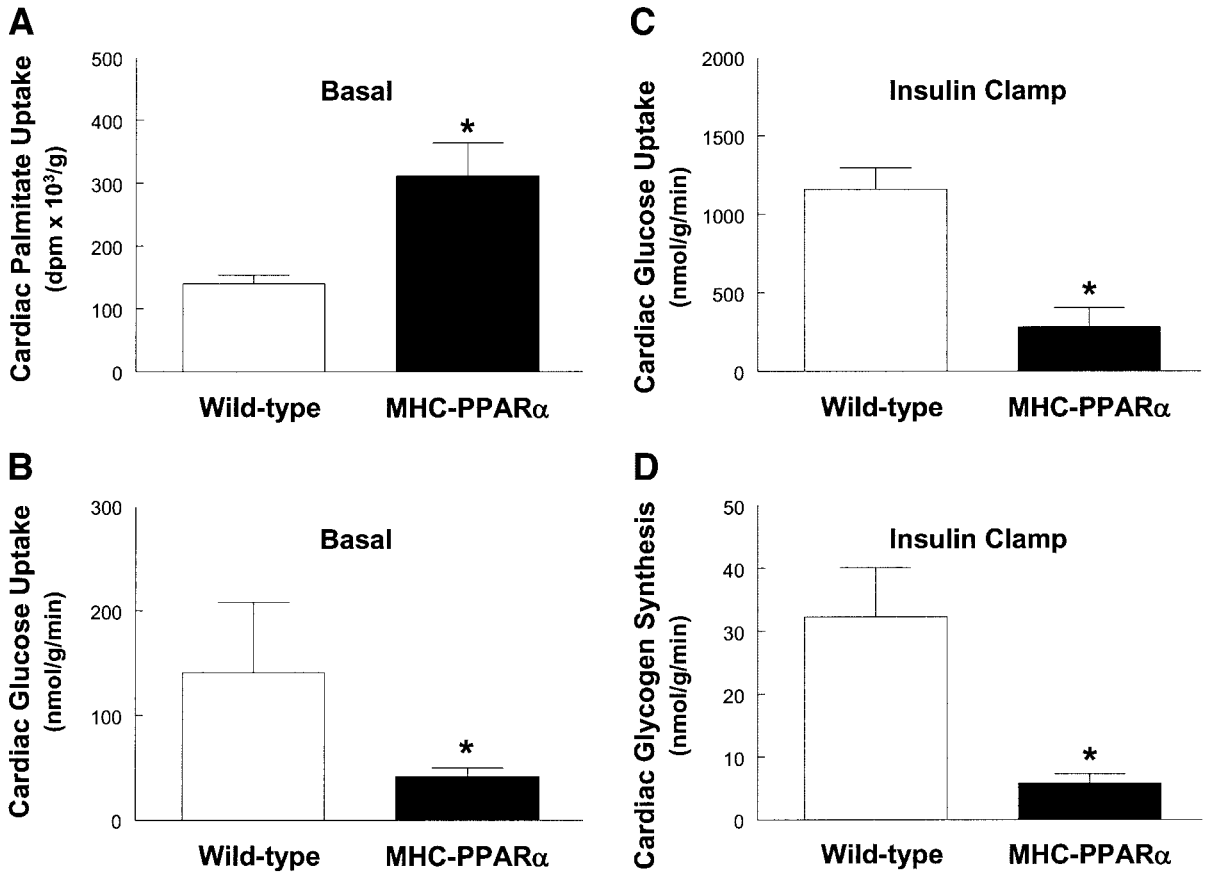

FIG. 1. Basal and insulin-stimulated cardiac palmitate uptake and glucose metabolism in vivo in the MHC-PPARα mice and wild-type littermates. *A*: Basal cardiac palmitate uptake. *B*: Basal cardiac glucose uptake. *C*: Insulin-stimulated cardiac glucose uptake during hyperinsulinemic-euglycemic clamps (insulin clamps). *D*: Insulin-stimulated cardiac glycogen synthesis during insulin clamps. Values are means ± SE for 6–7 experiments. *P < 0.05 vs. wild-type mice.

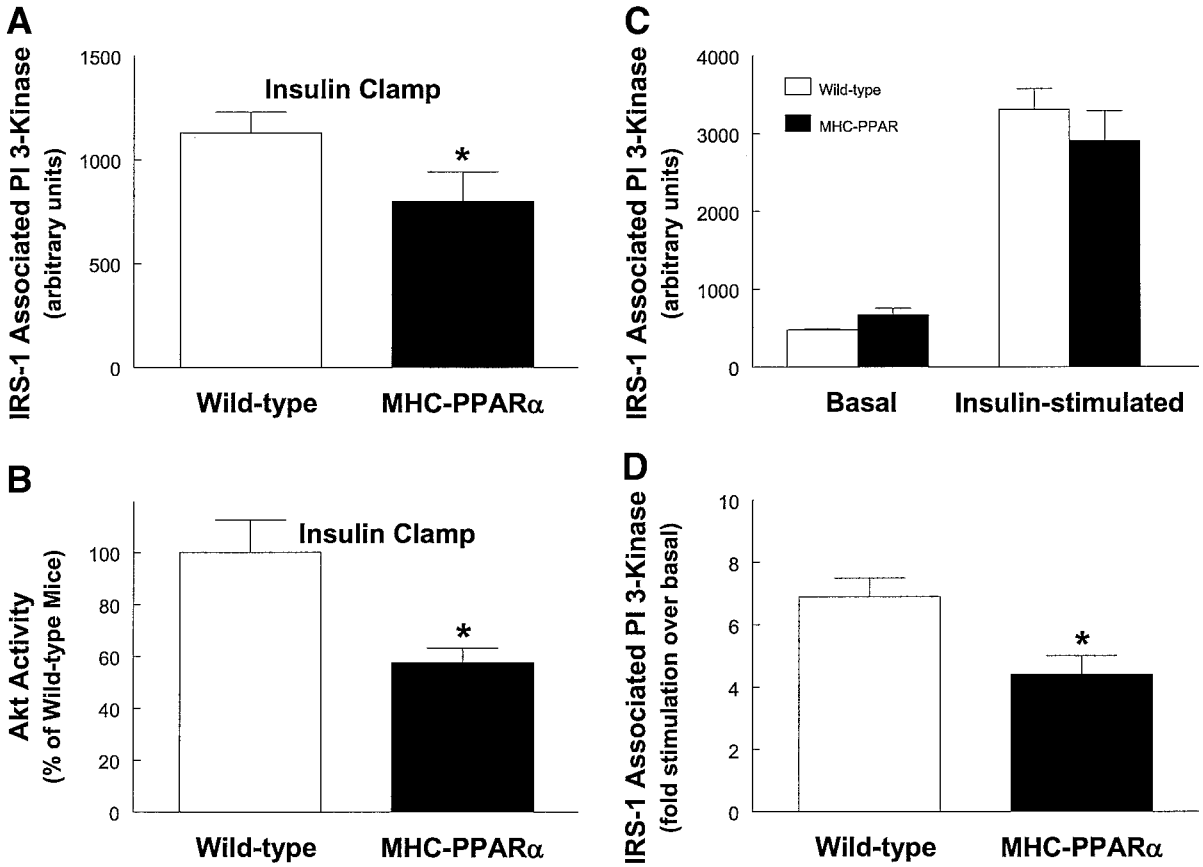

FIG. 2. Cardiac insulin signaling in vivo in the MHC-PPARα mice and wild-type littermates. *A*: Insulin-stimulated IRS-1–associated PI 3-kinase activity at the end of 2-h clamps. *B*: Insulin-stimulated Akt activity at the end of 2-h clamps. *C*: Basal and insulin-stimulated IRS-1–associated PI 3-kinase activity in heart following intraperitoneal injection of saline and insulin, respectively. *D*: Insulin-stimulated fold increase over basal in IRS-1–associated PI 3-kinase activity in heart. Values are means ± SE for 6–7 experiments. *$P < 0.05$ vs. wild-type mice.

Cardiac and hepatic metabolism in 8-week-old MHC-PPARα mice. To determine the mechanism of hepatic insulin resistance, hyperinsulinemic-euglycemic clamps were performed in additional groups of male MHC-PPARα mice and wild-type littermates at 8 weeks of age (n = 6–7). Basal Akt activities in heart were measured in overnight-fasted MHC-PPARα mice and wild-type littermates at ~8 weeks of age (n = 4 for each group). Echocardiography was performed to assess ventricular functions in additional group of 8-week-old male MHC-PPARα and wild-type mice (n = 5 for each group).

Statistical analysis. Data are expressed as means ± SE. The significance of the difference in mean values between wild-type mice versus MHC-PPARα mice was evaluated using the Student's t test. The statistical significance was at the $P < 0.05$ level, unless stated otherwise.

RESULTS

Basal cardiac energy metabolism in vivo. Whole-body lean and fat mass as well as overnight fasted plasma glucose and insulin levels did not differ between the male MHC-PPARα mice and wild-type littermates (12–14 weeks of age) (Table 1). To determine the effects of heart-selective overexpression of PPARα on basal cardiac energy metabolism in vivo, [^{14}C]palmitate was intravenously administered in awake mice. Basal palmitate uptake was increased by more than twofold in the MHC-PPARα mice (Fig. 1*A*), consistent with previous micro-PET measurement (10). Additionally, basal cardiac glucose uptake, as assessed using 2-[^{14}C]deoxyglucose, was reduced by 70% in the MHC-PPARα mice (Fig. 1*B*), also consistent with previous measurements using micro-PET and in isolated working hearts (10).

Cardiac insulin action and insulin signaling in vivo. Cardiac insulin signaling and insulin-stimulated glucose metabolism were assessed during a 2-h hyperinsulinemic-euglycemic clamp in awake mice. During the clamp experiments, plasma insulin concentration was raised to ~200 pmol/l, while the plasma glucose concentration was maintained at ~6 mmol/l by a variable infusion of glucose in both groups (Table 1). Insulin clamp increased cardiac glucose uptake by 10-fold in the wild-type mice compared with the basal state (Fig. 1*C*). In contrast, insulin-stimulated cardiac glucose uptake was significantly blunted in the MHC-PPARα mice (Fig. 1*C*), which was consistent with profoundly reduced GLUT4 content in the heart of MHC-PPARα mice (10). Defects in cardiac insulin action were further associated with an 80% decrease in insulin-stimulated glycogen synthesis in the heart of MHC-PPARα mice (Fig. 1*D*). Since glucose transport is a rate-controlling step in glucose utilization (23), decreases in insulin-stimulated glycogen synthesis may be partly accounted for by cardiac insulin resistance in the MHC-PPARα mice.

Previous studies (20,22) have shown that insulin resistance mediated by increased flux of fatty acids into skeletal muscle was secondary to alteration in insulin signaling activity. To determine whether cardiac insulin resistance in the MHC-PPARα mice was associated with defects in cardiac insulin signaling in vivo, we assessed insulin-stimulated activities of IRS-1–associated PI 3-ki-

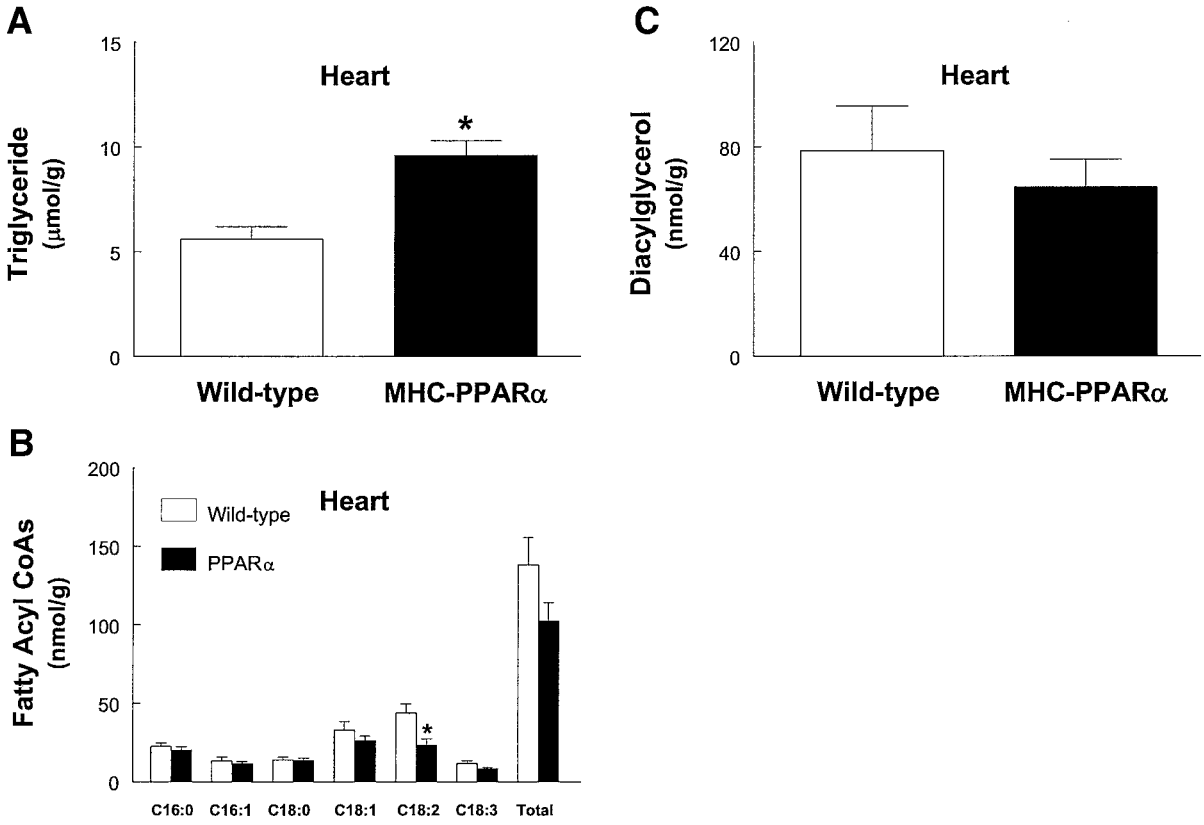

FIG. 3. Myocardial triglyceride and fatty acid metabolite levels in the MHC-PPARα mice and wild-type littermates. *A*: Myocardial triglyceride levels. *B*: Intramyocardial fatty acyl CoAs levels. *C*: Intramyocardial diacylglycerol levels. Values are means ± SE for 6–7 experiments. *$P < 0.05$ vs. wild-type mice.

nase and Akt, which are key intracellular mediators of insulin signaling (24,25), in tissues obtained at the end of 2-h insulin clamp experiments. Defects in insulin-mediated cardiac glucose metabolism were associated with 30–50% decreases in insulin-stimulated IRS-1–associated PI 3-kinase and Akt activity in the MHC-PPARα mice compared with the wild-type mice (Fig. 2*A* and *B*). Additionally, basal and insulin-stimulated IRS-1–associated PI 3-kinase activities in heart were assessed following intraperitoneal injection of insulin in another group of mice and showed no significant differences in the MHC-PPARα mice (Fig. 2*C*). However, insulin increased IRS-1–associated PI 3-kinase activity by approximately sevenfold over basal in the heart of wild-type mice, whereas insulin-mediated increase in IRS-1–associated PI 3-kinase activity over basal was significantly blunted in the heart of MHC-PPARα mice (approximately fourfold) (Fig. 2*D*). Basal Akt activity also showed a tendency to be reduced in the MHC-PPARα mice, although the difference did not reach statistical significance (data not shown). Altogether, these results suggest that cardiac insulin resistance in the MHC-PPARα mice may be attributed to both reduced GLUT4 contents and blunted insulin signaling activity.

Intramyocardial triglyceride and fatty acid metabolites. Since our recent studies demonstrated an important causative role of intracellular fatty acid–derived metabolites (i.e., fatty acyl CoA, diacylglycerol) on skeletal muscle insulin resistance (20,22), we assessed intramyocardial levels of triglyceride, fatty acyl CoAs, and diacylglycerol. Myocardial triglyceride levels were increased by twofold in the MHC-PPARα mice, which is consistent with increased lipid uptake in these mice (Fig. 3*A*). In contrast, individual and total (sum of C16:0, C16:1, C18:0, C18:1, C18:2, and C18:3) levels of intramyocardial fatty acyl CoAs were significantly (C18:2) or showed a tendency to be reduced in the MHC-PPARα mice (Fig. 3*B*). Consistent with the previous observation, intramyocardial levels of total diacylglycerol were not significantly altered in the MHC-PPARα mice (Fig. 3*C*).

Myocardial activity and expression of signaling proteins. Inoue et al. (26) have recently shown that liver-specific STAT3 knockout mice developed hepatic insulin resistance and suggested the role of STAT3 in hepatic glucose metabolism. Thus, we examined the expression of total STAT3 and insulin-stimulated STAT3 activity in the heart of MHC-PPARα mice. Interestingly, insulin-stimulated tyrosine phosphorylation of STAT3 was significantly reduced by 40% in the MHC-PPARα mice compared with the wild-type littermates, whereas total STAT3 expression levels were not altered in the MHC-PPARα mice (Fig. 4*A* and *C*). In contrast, myocardial activities of p38 MAPK, GSK3-α/-β, or expression of GSK3-β were not altered in the MHC-PPARα mice (Fig. 4*A* and *D*).

Hepatic and peripheral insulin action in vivo. We found that the steady-state rates of glucose infusion during clamp experiments were reduced by ~30% in the MHC-PPARα mice, reflecting whole-body insulin resistance in the MHC-PPARα mice (Fig. 5*A*). Basal HGP did not differ between the groups, but HGP during the insulin-stimulated state (clamps) was significantly increased in the MHC-

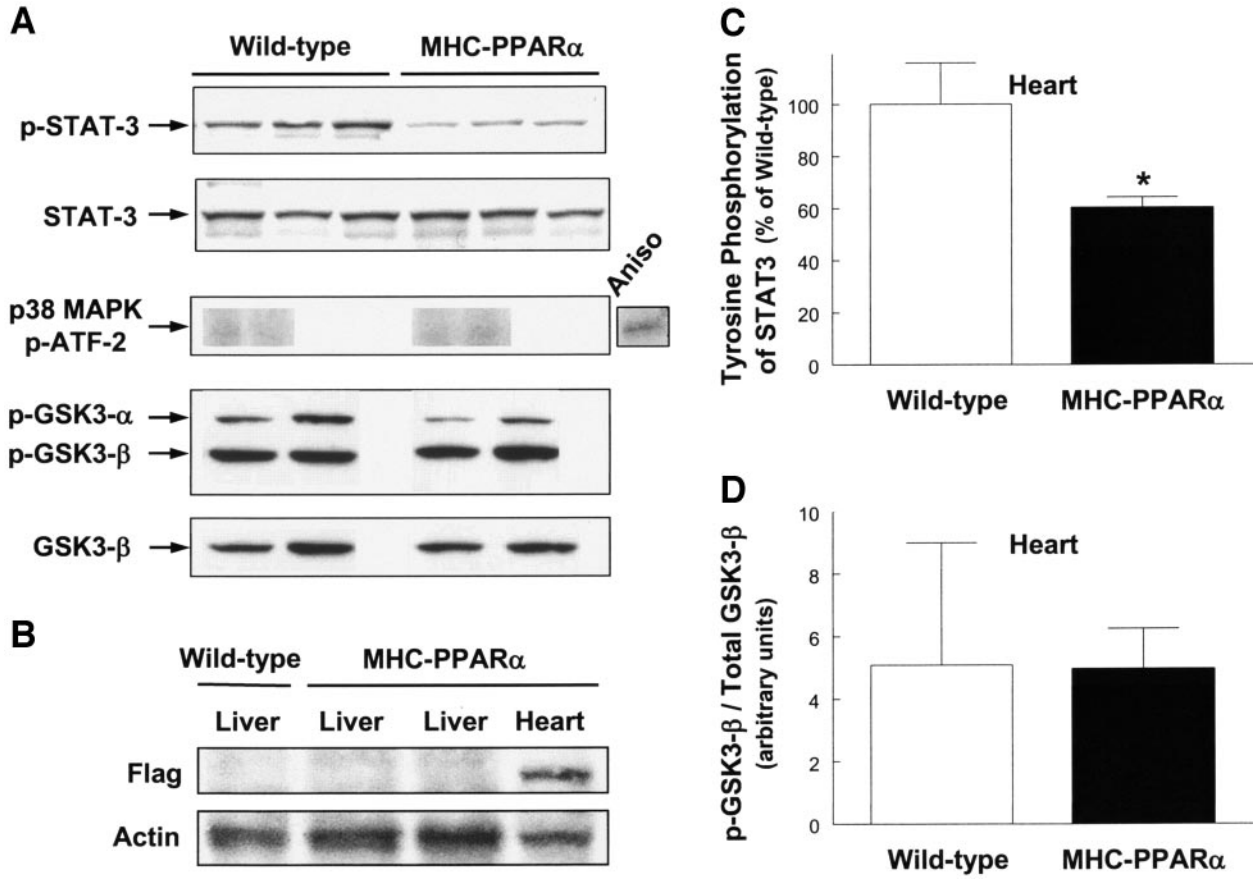

FIG. 4. Cardiac activity and expression of signaling proteins in the MHC-PPARα mice and wild-type littermates. *A*: Activity and expression pattern of STAT3, phospho-STAT3, p38 MAPK expressed as phospho-ATF-2, GSK3-β, and phospho-GSK3-α/-β. The positive control represents p38 MAPK activity measured from 293 cells stimulated with anisomycin (Aniso) for 30 min. *B*: Western blot of Flag epitope tag of PPARα in heart and liver. *C*: Insulin-mediated tyrosine phosphorylation of STAT3 in heart as expressed relative to the percentage of wild-type mice. *D*: Ratio of phospho-GSK3-β to total GSK3-β. Values are means ± SE for 6–7 experiments. *$P < 0.05$ vs. wild-type mice.

PPARα mice (Fig. 5*B*). As a result, hepatic insulin action, reflected as the insulin-mediated suppression of basal HGP, was markedly reduced in the MHC-PPARα mice compared with the wild-type littermates (Fig. 5*C*). In contrast, insulin-stimulated skeletal muscle glucose uptake was not altered in the MHC-PPARα mice (Fig. 5*D*). Additionally, insulin-stimulated whole-body glucose uptake and metabolic fluxes (i.e., glycolysis, glycogen plus lipid synthesis) were unaltered in the MHC-PPARα mice (data not shown). These findings indicate that the MHC-PPARα mice developed insulin resistance selectively in heart and liver, which accounted for the reduced glucose infusion rates during clamps in the MHC-PPARα mice.

Hepatic insulin resistance in the MHC-PPARα mice was associated with a 30% decrease in insulin-stimulated IRS-2–associated PI 3-kinase activity in the liver of MHC-PPARα mice (Fig. 6*A*). Similar to the findings in heart, hepatic triglyceride content was significantly elevated in the MHC-PPARα mice, whereas individual and total levels of intrahepatic fatty acyl CoAs were either significantly reduced or showed a tendency to be reduced in the MHC-PPARα mice (Fig. 6*B* and *C*). Additionally, intrahepatic total diacylglycerol levels were not altered in the MHC-PPARα mice (data not shown). In contrast to the findings in heart, insulin-mediated tyrosine phosphorylation of STAT3 was not altered in the liver of MHC-PPARα mice (data not shown). To determine whether altered hepatic lipid metabolism may be due to increased gene expression, we measured hepatic expression of PPARα and found no detectable levels of FLag PPARα in the liver of MHC-PPARα mice (Fig. 4*B*). Also, changes in the expression of endogenous PPARα were not detected in the MHC-PPARα mice (data not shown). Interestingly, circulating levels of IL-6 were increased by more than fourfold in the MHC-PPARα mice compared with the wild-type mice (~20 weeks of age) or both groups of mice at 8 weeks of age (Fig. 6*D*).

Glucose metabolism and cardiac function in the 8-week-old MHC-PPARα mice. To determine the mechanism of hepatic insulin resistance, hyperinsulinemic-euglycemic clamps were conducted in the MHC-PPARα mice and wild-type littermates at 8 weeks of age. The metabolic parameters (i.e., glucose, insulin) were comparable in the 8-week and the 12- to 14-week-old mice. Insulin-stimulated cardiac glucose uptake was reduced by ~60% in the 8-week-old MHC-PPARα mice compared with the age-matched wild-type mice (Fig. 7*A*), consistent with the notion that reduced glucose metabolism is secondary to PPARα-mediated alteration in lipid metabolism. Also, cardiac Akt activity was significantly reduced in the 8-week-old MHC-PPARα mice (1,541 ± 95 vs. 2,100 ± 167 arbitrary units in the age-matched wild-type mice, $P < 0.05$). In contrast, ventricular fractional shortening was not altered in the 8-week-old MHC-PPARα mice (Fig. 7*B*), suggesting

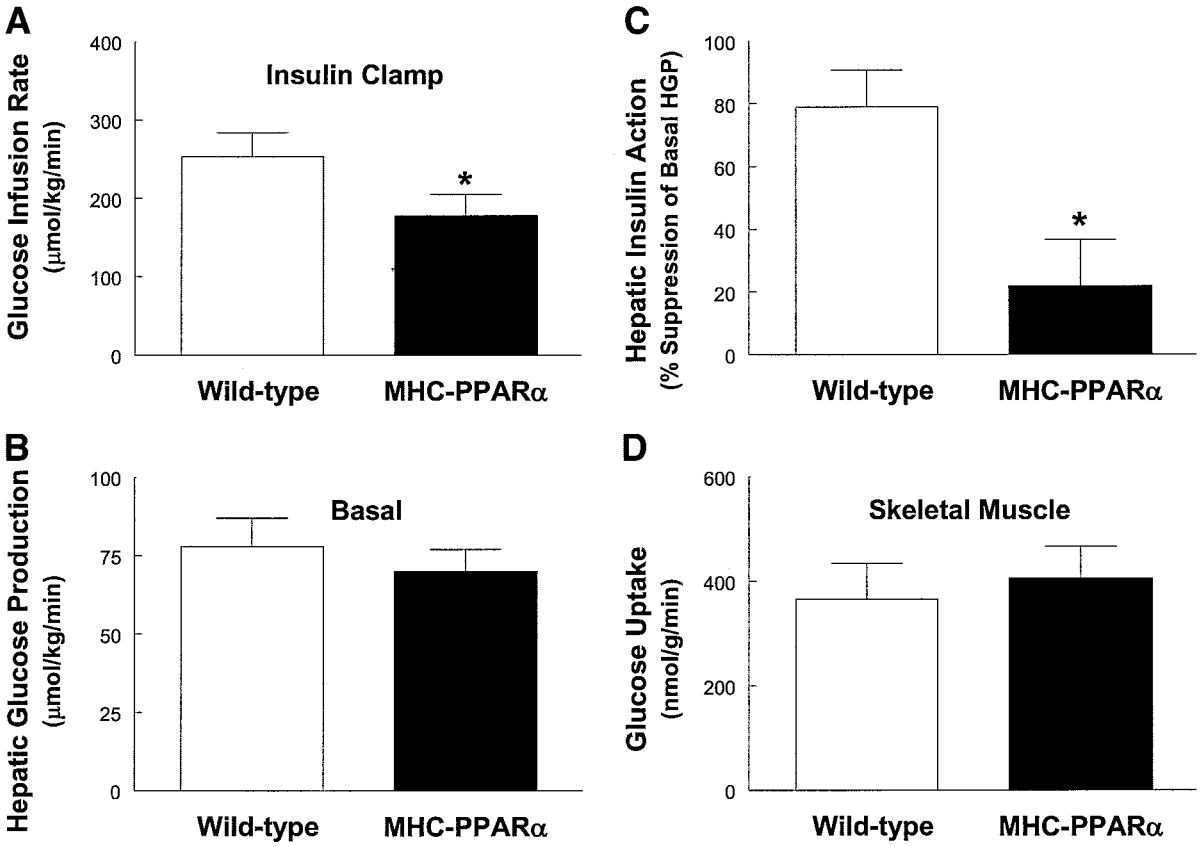

FIG. 5. Hepatic glucose metabolism and insulin action in vivo in the MHC-PPARα mice and wild-type littermates. *A*: Steady-state glucose infusion rate obtained from averaged rates of 90–120 min of hyperinsulinemic-euglycemic clamps. *B*: Basal hepatic glucose production. *C*: Hepatic insulin action as percent suppression of basal HGP. *D*: Insulin-stimulated glucose uptake in skeletal muscle during insulin clamps. Values are means ± SE for 6–7 experiments. **P* < 0.05 vs. wild-type mice.

that PPARα-induced metabolic changes in cardiomyocytes precede and are causally associated with altered cardiac function in the 12- to 14-week-old MHC-PPARα mice. Additionally, hepatic insulin action was normal in the 8-week-old MHC-PPARα mice (Fig. 7*C*), and this was associated with normal intrahepatic triglyceride content in these mice (Fig. 7*D*). These results are in contrast to the 12- to 14-week-old MHC-PPARα mice, which developed profound hepatic insulin resistance associated with elevated intrahepatic triglyceride content. Overall, these findings indicate that hepatic insulin resistance in the MHC-PPARα mice is age dependent and may be secondary to altered cardiac function in the MHC-PPARα mice.

DISCUSSION

Recent findings (3–5) indicate that the perturbation in cardiac energy metabolism and insulin resistance are among the earliest diabetes-induced events in the myocardium, preceding both functional and pathological changes. Studies (11,12) using isolated perfused heart preparations or cultured cardiomyocytes uniformly showed increased lipid oxidation in diabetic heart. Others (13,14) found markedly reduced rates of myocardial glucose uptake in type 2 diabetic subjects using PET combined with ^{18}F-fluoro-deoxy-glucose. The importance of cardiac insulin action and glucose metabolism was further demonstrated in mouse models of cardiac-specific ablation of GLUT4 or deletion of insulin receptor that developed cardiac hypertrophy and other metabolic phenotypes resembling diabetic heart (27–30). Additionally, mice with cardiac-specific overexpression of Akt were shown to develop ventricular hypertrophy associated with altered insulin signaling and glucose metabolism in the cardiomyocytes (31,32). Taken together, these findings indicate the important role of cardiac insulin resistance in the pathogenesis of diabetic heart failure.

Although increased lipid oxidation and reduced glucose metabolism are characteristic features of diabetic heart (3–5), it is unclear whether these changes are causally related. Our findings that basal cardiac glucose metabolism is reduced in the MHC-PPARα mice suggest that increased lipid oxidation, at least in part due to increased activity of PPARα, is causally associated with altered glucose metabolism in diabetic heart. More importantly, our results indicate that increased lipid oxidation may also be causally associated with reduced insulin action in the diabetic heart, and the mechanism may involve defects in cardiac insulin signaling activity and reduced GLUT4 contents (10). Previous studies indicated that IRS-1 and -2 are important intracellular mediators of insulin signaling and insulin-mediated glucose metabolism in skeletal muscle and liver, respectively (i.e., glucose transport and glycogen synthesis) (33). Defects in insulin-stimulated tyrosine phosphorylation of IRS-1 and -2 as well as IRS-associated PI 3-kinase were shown to mediate insulin resistance in skeletal muscle and liver, respectively (33). Additionally, mice lacking Akt2 (protein kinase B-β) were shown to develop whole-body insulin resistance (25). Our

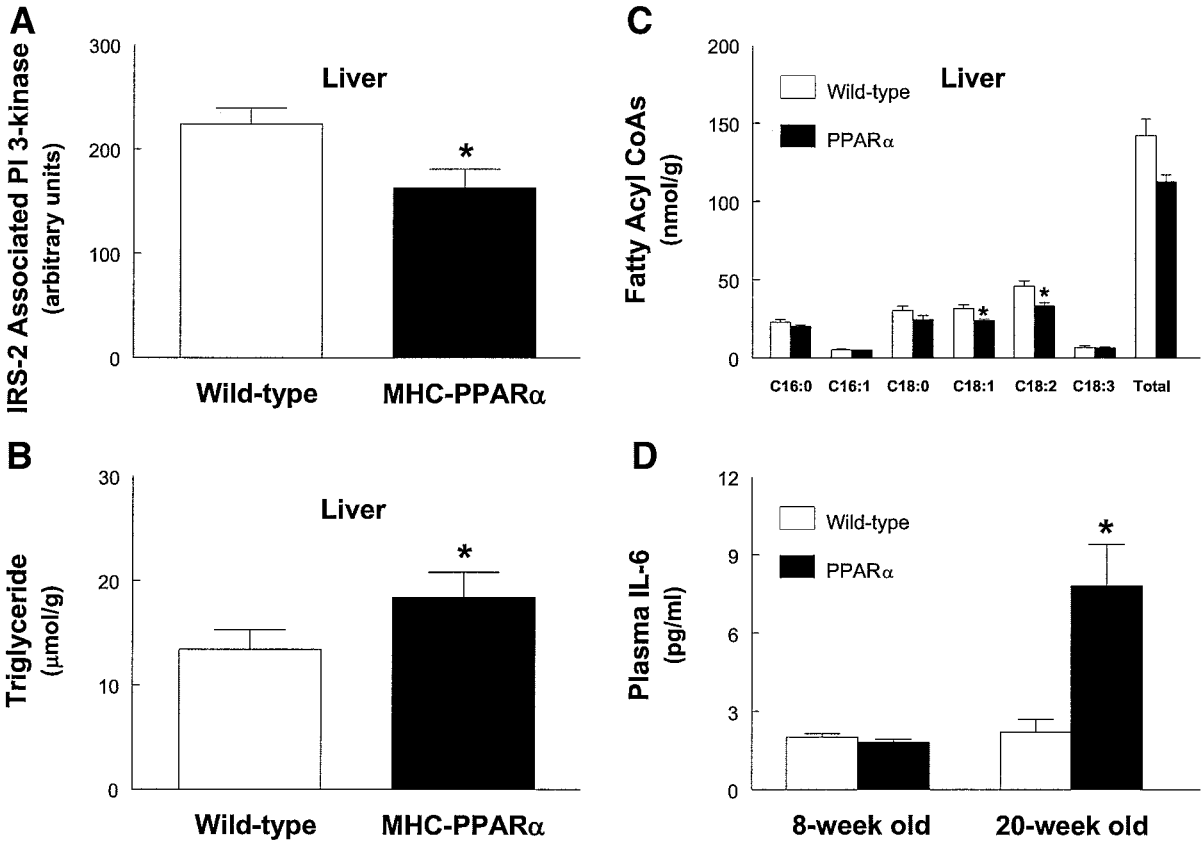

FIG. 6. Hepatic insulin signaling and fat content in the MHC-PPARα mice and wild-type littermates. *A*: Insulin-stimulated IRS-2–associated PI 3-kinase activity in liver. *B*: Hepatic triglyceride levels. *C*: Intrahepatic fatty acyl CoAs levels. *D*: Circulating IL-6 levels. Values are means ± SE for 6–7 experiments. *$P < 0.05$ vs. wild-type mice.

findings that insulin-stimulated activities of IRS-1–associated PI 3-kinase and Akt were markedly reduced in the MHC-PPARα mice implicate that defects in cardiac insulin signaling, in addition to reduced GLUT4 content (10), were responsible for reduced cardiac glucose metabolism in the MHC-PPARα mice.

The mechanism by which increased cardiac lipid metabolism causes defects in insulin signaling may involve intramyocardial accumulation of fatty acid–derived metabolites (i.e., fatty acyl CoA, diacylglycerol, ceramide) (34,35). The underlying mechanism may involve activation of serine kinase cascade, of which protein kinase C-θ and/or IκB kinase-β may play a role, by fatty acid metabolites leading to the serine phosphorylation of IRS-1 (35–37). In this regard, serine phosphorylation of IRS-1 has been shown to reduce tyrosine phosphorylation of IRS-1 and interfere with its ability to recruit and activate PI 3-kinase, as occurs upon treatment with tumor necrosis factor-α (38). However, despite increases in lipid oxidation, uptake, and myocardial triglyceride content, intracellular fatty acyl CoAs and diacylglycerol levels were not elevated in the MHC-PPARα mice. Instead, intramyocardial levels of fatty acid metabolites showed a tendency to be reduced in the MHC-PPARα mice, and this is consistent with previous findings (39) of unaltered ceramide content in the heart of MHC-PPARα mice. These results suggest that while such mechanism plays a role in fat-induced insulin resistance in skeletal muscle, it may not play a major role in the cardiac insulin resistance of MHC-PPARα mice. Additionally, paradoxical changes in myocardial triglyceride content and intracellular fatty acid metabolites suggest differential effects of PPARα on lipid uptake/synthesis and mitochondrial lipid oxidation. In other words, overexpression of PPARα may have caused a greater increase in mitochondrial lipid oxidation than lipid uptake, resulting in elevated triglyceride levels but unaltered fatty acyl CoAs. Although our findings contrast to the previously observed increases in triacylglycerol-containing long-chain fatty acid species in the heart of MHC-PPARα mice (39), the discrepancy may be due to the measurement taken in mice at a different age and/or metabolic state (i.e., fed versus fasted state).

A recent study (26) showed that liver-specific STAT3 knockout mice developed hepatic insulin resistance, suggesting a potential role of STAT3 in hepatic glucose metabolism. In this regard, the role of STAT3 on glucose metabolism has been recently identified in different mouse models of STAT3 deletion that have commonly shown alteration in glucose homeostasis (40,41). Since insulin-mediated tyrosine phosphorylation of STAT3 was significantly reduced in the MHC-PPARα mice, our results suggest the potential role of STAT3 in cardiac glucose metabolism and further indicate that blunted STAT3 activity may be responsible for cardiac insulin resistance in the MHC-PPARα mice (Fig. 8). Consistent with this notion, mice with cardiomyocyte-restricted knockout of STAT3 were shown to be more susceptible to cardiomyopathy following doxorubicin treatment (42), which may be due to altered glucose metabolism in these mice. In this regard, Hrelia et al. (43) showed that doxorubicin-induced cardio-

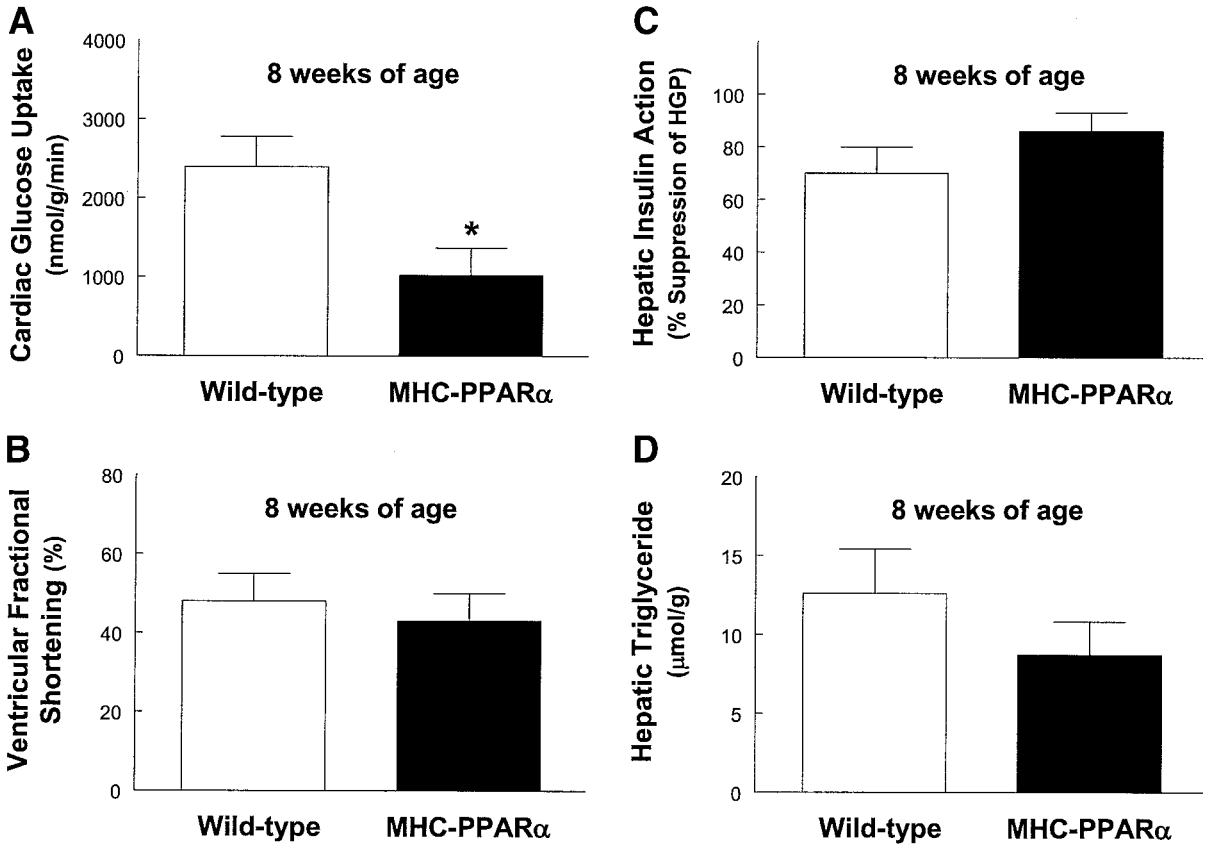

FIG. 7. Metabolic parameters in the MHC-PPARα mice and wild-type littermates at 8 weeks of age. *A*: Insulin-stimulated cardiac glucose uptake during hyperinsulinemic-euglycemic clamps. *B*: Ventricular fractional shortening. *C*: Hepatic insulin action. *D*: Hepatic triglyceride levels. Values are means ± SE for 6–7 experiments. *$P < 0.05$ vs. wild-type mice.

myopathy was associated with protective increases in glucose metabolism in cultured cardiomyocytes. Furthermore, recent studies (44–46) reported the antagonistic effects of and bidirectional regulation between STATs and PPARs and suggested a potential cross-talk between Janus kinase-STAT and PPAR pathways. Additionally, Gervois et al. (47) demonstrated a downregulation of STAT3 in liver following chronic treatment of the PPARα agonist, fenofibrate. Taken together, these findings indicate the important and novel role of STAT3 in cardiac glucose metabolism and that blunted STAT3 activity may partly mediate cardiac insulin resistance in the MHC-PPARα mice. Importantly, our findings also suggest that the reciprocal regulation between PPARα and STAT3 may be the mechanism by which increased cardiac lipid oxidation leads to insulin resistance in the MHC-PPARα mice (Fig. 8). Alternatively, cardiac insulin resistance may be due to prolonged state of high lipid oxidation in the heart of MHC-PPARα mice that leads to accumulation of other lipid intermediates, mitochondrial or peroxisomal generation of reactive oxygen species, or excessive oxygen consumption (48–50).

Surprisingly, MHC-PPARα mice developed defects in hepatic insulin action associated with blunted IRS-2–associated PI 3-kinase activity in liver. Hepatic insulin resistance may be due to increased intrahepatic triglyceride content in the MHC-PPARα mice (20). Since heart is a major organ for fatty acid clearance (51), increased cardiac lipid oxidation in the MHC-PPARα mice may alter hepatic lipid metabolism in order to meet the increasing demand of the transgenic heart (Fig. 8). This may be reflected by a tendency for reduced intrahepatic total fatty acyl CoAs and significantly reduced intrahepatic levels of C18:1 and C18:2 in the MHC-PPARα mice. To further determine the mechanism of hepatic insulin resistance in the MHC-PPARα mice, we assessed cardiac insulin action, function, and hepatic glucose/lipid metabolism in the 8-week-old mice. Insulin-stimulated cardiac glucose uptake was similarly reduced in the 8-week-old MHC-PPARα mice compared with the 12- to 14-week-old MHC-PPARα mice. Despite early changes in cardiac glucose metabolism, ventricular fractional shortening was not altered in the 8-week-old MHC-PPARα mice. These results indicate that cardiac insulin resistance and blunted glucose metabolism developed before the onset of cardiac dysfunction in the MHC-PPARα mice. Our findings further support the notion that altered cardiac energy metabolism may precede and cause changes in function of diabetic heart. Moreover, hepatic insulin action was normal in the 8-week-old MHC-PPARα mice, which was associated with normal hepatic triglyceride content. The observation of age dependence in the development of hepatic insulin resistance in the MHC-PPARα mice as well as overlapping pattern of blunted cardiac function and hepatic glucose metabolism further supports the causal relationship between heart and liver. In this regard, the scenario involving potential cross-talk between heart and liver may be mediated by circulating inflammatory cytokines, such as IL-6 (Fig. 8). Our findings that circulating IL-6 levels were not altered in the MHC-PPARα mice at 8 weeks of age but

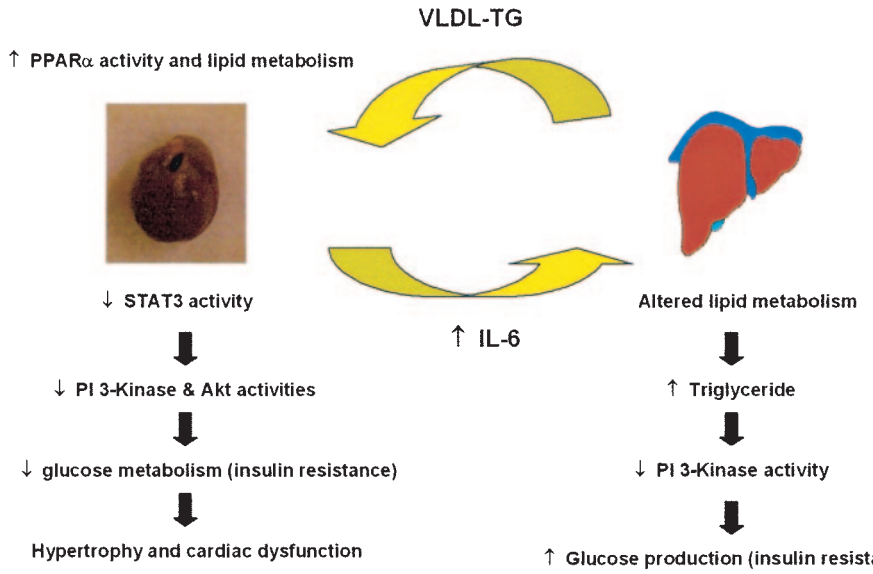

FIG. 8. Diagram depicting the scenario of events in the development of insulin resistance in heart and liver of MHC-PPARα mice.

significantly elevated at ~20 weeks of age, when cardiac dysfunction was evident, suggest the physiological role of IL-6 in the MHC-PPARα mice. In this regard, IL-6 and tumor necrosis factor-α have been shown to be secreted by cardiomyocytes and in failing heart (52,53). Altogether, more studies are clearly needed to examine the cross-talk relationship between the heart and liver and to determine the underlying mechanism.

In summary, heart-specific overexpression of PPARα caused early defects in cardiac glucose metabolism and insulin resistance that led to ventricular hypertrophy and blunted cardiac functions. Cardiac insulin resistance was associated with reduced STAT3, IRS-1–associated PI 3-kinase, and Akt activities, suggesting the possible role of STAT3 in modulating cardiac glucose metabolism. Furthermore, age-associated development of hepatic insulin resistance in the MHC-PPARα mice may be due to altered cardiac metabolism, function, and/or IL-6 level. Overall, our results demonstrate the important role of cardiac energy metabolism in the development of diabetic heart failure and provide novel insights into the potential cross-talk between heart and liver.

ACKNOWLEDGMENTS

This study is supported by grants from the U.S. Public Health Service (U24 DK-59635 to J.K.K. and HL-04429 to K.S.R.), American Diabetes Association (7-01-JF-05 and 1-04-RA-47 to J.K.K. and 7-02-JF-26 to Y.-B.K.), The Robert Leet and Clara Guthrie Patterson Trust Award to J.K.K., and American Heart Association to K.S.R.

We are grateful to Dongyan Zhang, Anthony Romanneli, Aida Groszmann, and Jonas Lai for technical assistance.

REFERENCES

1. Stamler J, Vaccaro O, Neaton JD, Wentworth D: Diabetes, other risk factors, and 12-yr cardiovascular mortality for men screened in the Multiple Risk Factor Intervention Trial. *Diabetes Care* 16:434–444, 1993
2. Taegtmeyer H, Razeghi P: Heart disease in diabetes: resist the beginnings (Letter). *J Am Col Cardiology* 43:315, 2004
3. Rodrigues B, McNeill JH: The diabetic heart: metabolic causes for the development of a cardiomyopathy. *Cardiovascular Res* 26:913–922, 1992
4. Taegtmeyer H, Passmore JM: Defective energy metabolism of the heart in diabetes. *Lancet* 1:139–141, 1985
5. Lopaschuk GD: Abnormal mechanical function in diabetes: relationship to altered myocardial carbohydrates/lipid metabolism. *Coronary Artery Dis* 7:116–123, 1996
6. Rosen ED, Spiegelman BM: PPARγ: a nuclear regulator of metabolism, differentiation, and cell growth. *J Biol Chem* 276:37731–37734, 2001
7. Berger J, Moller DE: The mechanisms of action of PPARs. *Annu Rev Med* 53:409–435, 2002
8. Taegtmeyer H: Energy metabolism of the heart: from basic concepts to clinical applications. *Curr Prob Cardiol* 19:59–113, 1994
9. Barger PM, Kelly DP: PPAR signaling in the control of cardiac energy metabolism. *Trends Cardiovasc Med* 10:238–245, 2002
10. Finck BN, Lehman JJ, Leone TC, Welch MJ, Bennett MJ, Kovacs A, Han X, Gross RW, Kozak R, Lopaschuk GD, Kelly DP: The cardiac phenotype induced by PPARα overexpression mimics that caused by diabetes mellitus. *J Clin Invest* 109:121–130, 2002
11. Schaffer SW, Seyed-Mozaffari M, Cutcliff CR, Wilson GL: Postreceptor myocardial metabolic defect in a rat model of non-insulin-dependent diabetes mellitus. *Diabetes* 35:593–597, 1986
12. Kolter T, Uphues I, Eckel J: Molecular analysis of insulin resistance in isolated ventricular cardiomyocytes of obese Zucker rats. *Am J Physiol* 273:E59–E67, 1997
13. Yokoyama I, Yonekura K, Ohtake T, Kawamura H, Matsumoto A, Inoue Y, Aoyagi T, Sugiura S, Omata M, Ohtomo K, Nagai R: Role of insulin resistance in heart and skeletal muscle F-18 fluorodeoxyglucose uptake in patients with non-insulin-dependent diabetes mellitus. *J Nucl Cardiol* 7:242–248, 2000
14. Iozzo P, Chareonthaitawee P, Dutka D, Betteridge DJ, Ferrannini E, Camici PG: Independent association of type 2 diabetes and coronary artery disease with myocardial insulin resistance. *Diabetes* 51:3020–3024, 2002
15. Voipio-Pulkki LM, Nuutila P, Kuuti MJ, Ruotsalainen U, Haaparanta M, Teras M, Wegelius U, Koivisto VA: Heart and skeletal muscle glucose disposal in type 2 diabetic patients as determined by positron emission tomography. *J Nucl Med* 34:2064–2067, 1993
16. Kim HJ, Higashimori T, Park SY, Choi H, Dong J, Kim YJ, Noh HL, Cho YR, Cline G, Kim YB, Kim JK: Differential effects of interleukin-6 and -10 on skeletal muscle and liver insulin action in vivo. *Diabetes* 53:1060–1067, 2004
17. Kim YB, Shulman GI, Kahn BB: Fatty acid infusion selectively impairs insulin action on Akt1 and protein kinase C λ/ζ but not on glycogen synthase. *J Biol Chem* 277:32915–32922, 2002
18. Cresci S, Wright LD, Spratt JA, Briggs FN, Kelly DP: Activation of a novel metabolic gene regulatory pathway by chronic stimulation of skeletal muscle. *Am J Physiol* 270:C1413–C1420, 1996
19. Wu JJ, Bennett AM: Essential role for mitogen-activated protein (MAP) kinase phosphatase-1 in stress-responsive MAP kinase and cell survival signaling. *J Biol Chem* 280:16461–16466, 2005
20. Kim JK, Fillmore JJ, Chen Y, Yu C, Moore IK, Pypaert M, Lutz EP, Kako Y,

Velez-Carrasco W, Goldberg IJ, Breslow JL, Shulman GI: Tissue-specific overexpression of lipoprotein lipase causes tissue-specific insulin resistance. *Proc Natl Acad Sci U S A* 98:7522–7527, 2001
21. Bligh EG, Dyer WJ: A rapid method of total lipid extraction and purification. *Can J Biochem Physiol* 37:911–917, 1959
22. Yu C, Chen Y, Cline GW, Zhang D, Zong H, Wang Y, Bergeron R, Kim JK, Cushman SW, Cooney GJ, Atcheson B, White MF, Kraegen EW, Shulman GI: Mechanism by which fatty acids inhibit insulin activation of insulin receptor substrate-1 (IRS-1)-associated phosphatidylinositol 3-kinase activity in muscle. *J Biol Chem* 277:50230–50236, 2002
23. Ren JM, Marshall BA, Gulve EA, Gao J, Johnson, DW, Holloszy JO, Mueckler M: Evidence from transgenic mice that glucose transport is rate-limiting for glycogen deposition and glycolysis in skeletal muscle. *J Biol Chem* 268:16113–16115, 1993
24. Previs SF, Withers DJ, Ren J-M, White MF, Shulman GI: Contrasting effects of IRS-1 versus IRS-2 gene disruption on carbohydrate and lipid metabolism in vivo. *J Biol Chem* 275:38990–38994, 2000
25. Cho H, Mu J, Kim JK, Thorvaldsen JL, Chu Q, Crenshaw III EB, Kaestner KH, Bartolomei MS, Shulman GI, Birnbaum MJ: Insulin resistance and diabetes mellitus-like syndrome in mice lacking Akt2 (PKBβ). *Science* 292:1728–1731, 2001
26. Inoue H, Ogawa W, Ozaki M, Haga S, Matsumoto M, Furukawa K, Hashimoto N, Kido Y, Mori T, Sakaue H, Teshigawara K, Jin S, Iguchi H, Hiramatsu R, LeRoith D, Takeda K, Akira S, Kasuga M: Role of STAT-3 in regulation of hepatic gluconeogenic genes and carbohydrate metabolism in vivo. *Nat Med* 10:168–174, 2004
27. Katz BB, Stenbit AE, Hatton K, DePinho R, Charron MJ: Cardiac and adipose tissue abnormalities but not diabetes in mice deficient in GLUT4. *Nature* 377:151–155, 1995
28. Abel ED, Kaulbach HC, Tian R, Hopkins JC, Duffy J, Doetschman T, Minnemann T, Boers ME, Hadro E, Oberste-Berghaus C, Quist W, Lowell BB, Ingwall JS, Kahn BB: Cardiac hypertrophy with preserved contractile function after selective deletion of GLUT4 from the heart. *J Clin Invest* 104:1703–1714, 1999
29. Stenbit AE, Tsao TS, Li J, Burcelin R, Geenen DL, Factor SM, Houseknecht K, Katz EB, Charron MJ: GLUT4 heterozygous knockout mice develop muscle insulin resistance and diabetes. *Nat Med* 3:1096–1101, 1997
30. Belke DD, Betuing S, Tuttle MJ, Graveleau C, Young ME, Pham M, Zhang D, Cooksey RC, McClain DA, Litwin SE, Taegtmeyer H, Severson D, Kahn CR, Abel ED: Insulin signaling coordinately regulates cardiac size, metabolism, and contractile protein isoforms expression. *J Clin Invest* 109:629–639, 2002
31. Matsui T, Li L, Wu JC, Cook SA, Nagoshi T, Picard MH, Liao R, Rosenzweig A: Phenotypic spectrum caused by transgenic overexpression of activated Akt in the heart. *J Biol Chem* 277:22896–22901, 2002
32. Nagoshi T, Matsui T, Champion HC, Li L, Rosenzweig A: Adenoviral expression of activated PI3-kinase rescues detrimental effects of chronic cardiac-specific Akt activation. *Circulation* 110:III-285, 2004
33. Kahn CR: Banting Lecture: Insulin action, diabetogenes, and the cause of type II diabetes. *Diabetes* 43:1066–1084, 1994
34. Unger RH, Orci L: Lipoapoptosis: its mechanism and its diseases. *Biochim Biophys Acta* 1585:202–212, 2002
35. Shulman GI: Cellular mechanisms of insulin resistance. *J Clin Invest* 106:171–176, 2000
36. Yuan M, Konstantopoulos N, Lee J, Hansen L, Li ZW, Karin M, Shoelson SE: Reversal of obesity- and diet-induced insulin resistance with salicylates or targeted disruption of IKK-beta. *Science* 293:1673–1677, 2001
37. Kim JK, Fillmore JJ, Sunshine MJ, Albrecht B, Higashimori T, Kim D-W, Liu Z-X, Soos TJ, Cline GW, O'Brien WR, Littman DR, Shulman GI: PKC-θ knockout mice are protected from fat-induced insulin resistance. *J Clin Invest* 114:823–827, 2004
38. Rui L, Aguirre V, Kim JK, Shulman GI, Lee A, Corbould A, Dunaif A, White MF: Insulin/IGF-1 and TNF-α stimulate phosphorylation of IRS-1 at inhibitory Ser^{307} via distinct pathways. *J Clin Invest* 107:181–189, 2001
39. Finck BN, Han X, Courtois M, Aimond F, Nerbonne JM, Kovacs A, Gross RW, Kelly DP: A critical role for PPARα-mediated lipotoxicity in the pathogenesis of diabetic cardiomyopathy: modulation by dietary fat content. *Proc Natl Acad Sci U S A* 100:1226–1231, 2003
40. Cui Y, Huang L, Elefteriou F, Yang G, Shelton JM, Giles JE, Oz OK, Pourbahrami T, Lu CY, Richardson JA, Karsenty G, Li C: Essential role of STAT3 in body weight and glucose homeostasis. *Mol Cell Biol* 24:258–269, 2004
41. Mattson MP: Lose weight STAT: CNTF tops leptin. *Trends Neurosci* 24:313–314, 2001
42. Jacoby JJ, Kalinowski A, Liu MG, Zhang SS, Gao Q, Chai GX, Ji L, Iwamoto Y, Li E, Schneider M, Russell KS, Fu X-Y: Cardiomyocyte-restricted knockout of STAT3 results in higher sensitivity to inflammation, cardiac fibrosis, and heart failure with advanced age. *Proc Natl Acad Sci U S A* 100:12929–12934, 2003
43. Hrelia S, Fiorentini D, Maraldi T, Angeloni C, Bordoni A, Biagi PL, Hakim G: Doxorubicin induces early lipid peroxdation associated with changes in glucose transport in cultured cardiomyocytes. *Biochim Biophys Acta* 1567:150–156, 2002
44. Zhou Y-C, Waxman DJ: Cross-talk between Janus kinase-signal transducer and activator of transcription (JAK-STAT) and peroxisome proferator-activated receptor-α (PPAR α) signaling pathways. *J Biol Chem* 274:2672–2681, 1999
45. Shipley JM, Waxman DJ: Down-regulation of STAT5b transcriptional activity by ligand-activated peroxisome proliferator-activated receptor (PPAR) α and PPARγ. *Mol Pharmacol* 64:355–364, 2003
46. Zhou YC, Waxman DJ: STAT5b down-regulates peroxisome proliferator-activated receptor α transcription by inhibition of ligand-dependent activation function region-1 trans-activation domain. *J Biol Chem* 274:29874–29882, 1999
47. Gervois P, Kleemann R, Pilon A, Percevault F, Koenig W, Staels B, Kooistra T: Global suppression of IL-6-induced acute phase response gene expression after chronic in vivo treatment with the peroxisome proliferator-activated receptor-α activator fenofibrate. *J Biol Chem* 279:16154–16160, 2004
48. Kaul N, Siveski-Illiskovic N, Hill M, Khaper N, Seneviratne C, Singal PK: Probucol treatment reverses antioxidant and functional deficit in diabetic cardiomyopathy. *Mol Cell Biochem* 42:283–288, 1996
49. Zhou YT, Grayburn P, Karim A, Shimabukuro M, Higa M, Baetens D, Orci L, Unger RH: Lipotoxic heart disease in obese rats: implications for human obesity. *Proc Natl Acad Sci U S A* 97:1784–1789, 2000
50. Chiu H-C, Kovaes A, Ford DA, Hsu F-F, Garcia R, Herrero P, Saffitz JE, Schaffer JE: A novel mouse model of lipotoxic cardiomyopathy. *J Clin Invest* 107:813–822, 2001
51. Augustus A, Yagyu H, Haemmerle G, Bensadoun A, Vikramadithyan RK, Park S-Y, Kim JK, Zechner R, Goldberg IJ: Cardiac-specific knock-out of lipoprotein lipase alters plasma lipoprotein triglyceride metabolism and cardiac gene expression. *J Biol Chem* 279:25050–25057, 2004
52. Gwechenberger M, Mendoza LH, Youker KA, Frangogiannis NG, Smith CW, Michael LH, Entman ML: Cardiac myocytes produce interleukin-6 in culture and in viable border zone of reperfused infarctions. *Circulation* 99:546–551, 1999
53. Hogye M, Mandi Y, Csanady M, Sepp R, Buzas K: Comparison of circulating levels of interleukin-6 and tumor necrosis factor-alpha in hypertrophic cardiomyopathy and in idiopathic dilated cardiomyopathy. *Am J Cardiol* 94:249–251, 2004